Magn Reson Med Sci 2024; 23; 127–135
doi:10.2463/mrms.mp.2022-0067 Published Online: January 24, 2023

MAJOR PAPER

MR Imaging Findings of Uterine Adenomatoid Tumors

Mayumi Takeuchi[1*], Kenji Matsuzaki[2], Yoshimi Bando[3], and Masafumi Harada[1]

Purpose: Adenomatoid tumor is a rare benign genital tract neoplasm of mesothelial origin. Uterine adenomatoid tumors occur in the outer myometrium and may mimic leiomyomas. Because hormonal treatment is not applicable to adenomatoid tumors and laparoscopic enucleation is not easy as myomectomy, it is important to differentiate adenomatoid tumors from leiomyomas for the adequate treatment. The purpose of this study is to evaluate the MRI findings of adenomatoid tumor for the differentiation from leiomyoma.

Methods: MRI findings of surgically proven 10 uterine adenomatoid tumors in 9 women were retrospectively evaluated with correlation to histopathological findings.

Results: All 10 tumors appeared as solid myometrial masses and showed heterogeneous signal intensity with admixture of partially ill-defined slight high-intensity areas containing abundant tubular tumor cells and well-defined myoma-like low-intensity areas reflecting smooth muscle hypertrophy on T2WI including 4 lesions with peripheral ring-like high intensity. High-intensity areas on T2WI tended to show high intensity on diffusion-weighted imaging (DWI) with relatively high apparent diffusion coefficient (ADC), suggesting T2 shine-through effect due to abundant tubules. Intra-tumoral hemorrhage revealed on MRI was rare. Early intense contrast-enhanced areas on dynamic contrast-enhanced study were observed dominantly within the high-intensity areas but rarely within the low-intensity areas on T2WI.

Conclusion: The outer myometrial mass with the admixture of well-defined low- and ill-defined high-intensity areas on T2WI may be suggestive of adenomatoid tumor. Peripheral ring-like high intensity on T2WI and DWI may also be suggestive. Dynamic contrast-enhanced MR study may be helpful for the differentiation from leiomyoma.

Keywords: *adenomatoid tumor, diffusion weighted imaging, dynamic contrast-enhanced-magnetic resonance imaging, magnetic resonance imaging, uterus*

Introduction

Adenomatoid tumor, which was first described in 1945 by Golden and Ash, is a rare benign genital tract neoplasm of mesothelial origin, and commonly affects the fallopian tubes and the uterus in the female pelvis. Adenomatoid tumor arising from the uterus typically occurs in women of reproductive age, and is found in 1%–5% of hysterectomy specimens. Uterine adenomatoid tumor is usually located in the outer myometrium, and typically a small solid mass measuring 0.5–1 cm in diameter but occasionally larger, or may be cystic.[1–6] Most of the uterine adenomatoid tumor may be misdiagnosed as a leiomyoma because it shares the similar imaging features of leiomyomas.[7–9] Because leiomyoma is sensitive for hormone therapy, unnecessary hormone therapy may be administered for adenomatoid tumor which is misdiagnosed as leiomyoma.[7,9] In addition, because adenomatoid tumor is densely adherent to the surrounding myometrium without capsule, it may be difficult to enucleate and surgeons should modify the procedure during laparoscopic tumor resection under the diagnosis of leiomyoma.[10,11] Therefore, it is important to differentiate adenomatoid tumor from leiomyoma for the adequate treatment. The purpose of this study is to evaluate the MRI findings of adenomatoid tumor for the differentiation from leiomyoma.

[1]Department of Radiology, Tokushima University, Tokushima, Tokushima, Japan
[2]Department of Radiological Technology, Tokushima Bunri University, Sanuki, Kagawa, Japan
[3]Division of Pathology, Tokushima University Hospital, Tokushima, Tokushima, Japan

*Corresponding author: Department of Radiology, Tokushima University, 3-18-15, Kuramotocho, Tokushima, Tokushima 770-8503, Japan. Phone: 81-88-633-9283, Fax: 81-88-633-7468, E-mail: mayumi@tokushima-u.ac.jp

Received: June 7, 2022 | Accepted: November 10, 2022

Materials and Methods

Patients

The institutional review board in our hospital approved this retrospective study, and waived the requirement for written informed consent of patients. We cross-referenced the database of the Department of Radiology and the Division of Pathology to identify all patients with histologically proven adenomatoid tumor of the uterus who had undergone MRI examinations between April 2010 and August 2019. A total of 18 uterine adenomatoid tumors in 17 patients were extracted from the database of the Division of Pathology. Two lesions in two patients were excluded because MRI examination was not performed. In 16 lesions in 15 patients for which MRI examination was performed, 6 lesions in 6 patients were excluded in the current study. Two lesions in two patients were small, only a few millimeters in size, making adequate evaluation by MR imaging difficult. Four lesions in four patients were associated with multiple leiomyomas, and it was not possible to accurately identify which mass depicted on MR images was an adenomatoid tumor. In 10 lesions in 9 patients (29–54 years of age, mean 42 years), MR imaging findings could be evaluated with correlation to histopathological findings and were included in this study. The preoperative diagnosis was leiomyoma in all cases, with degenerative leiomyoma, variants of leiomyoma, or smooth muscle tumor of uncertain malignant potential (STUMP) as differential diagnoses. Tumorectomy was performed in 5 patients, and total hysterectomy was performed in 4 patients (all 4 patients were over 40 years of age with no desire for childbearing).

MR imaging

MRI examinations were performed with 3T (one patient by Signa HDxt 3.0T; GE Healthcare, Milwaukee, WI, USA, one patient by Discovery MR750; GE Healthcare) or 1.5T (three patients by Signa Explorer; GE Healthcare, two patients by Signa Excite; GE Healthcare, one patient by Signa HDxt 1.5T; GE Healthcare, one patient by MRT200PP3; Toshiba Medical Systems, Tochigi, Japan) superconducting MRI systems before surgery. Sagittal and axial fast spin-echo T2-weighted images (TR, 3500–7000 milliseconds; TE, 94–125.8 milliseconds), and axial fast spin-echo (TR, 516.7–720 milliseconds; TE, 7.9–15 milliseconds) or gradient-echo (TR, 7.3–7.8 milliseconds; TE, 3.1 milliseconds) T1-weighted images with or without fat-saturation were obtained in all 9 patients. Scan parameters of T1- and T2-weighted images varied because images were obtained with multiple MR devices. Gadolinium-enhanced T1-weighted images with fat-saturation were obtained after administration of a gadolinium chelate (0.1 mmol per kilogram of body weight) in 7 lesions in 6 patients including 6 lesions in 5 patients with dynamic contrast-enhanced study. Diffusion-weighted imaging (DWI) (TR, 4000–10000 milliseconds; TE, 55.9–76.5 milliseconds; $b = 800 s/mm^2$) was obtained in 9 lesions in 8 patients. T2*-based 3D gradient echo susceptibility-weighted sequence using multiple magnitude images with different TEs for the image generation (susceptibility-weighted angiography [SWAN]; TR, 40–78.8 milliseconds; TE, 23.7–49.2 milliseconds) was obtained in 6 lesions in 5 patients.

Analysis methods

Two radiologists both with more than 20 years of experiences of gynecologic MRI qualitatively evaluated the images: location, shape, size, margin, signal intensity compared to the outer myometrium on T1-weighted image with or without contrast enhancement, T2-weighted image, DWI ($b = 800 s/mm^2$), and computed DWI ($b = 1500 s/mm^2$); the presence of hemorrhagic foci (high intensity on T1-weighted image and/or signal voids on SWAN). The reviewers examined all images of the cases independently and then resolved discrepancies by consensus. The mean apparent diffusion coefficient (ADC) values were measured in circular ROIs within a mass (entire mass, high-intensity area, and low-intensity area on DWI, respectively) from ADC maps generated by using b-values of 0 and 800 s/mm^2 on the workstation (AW4.2; GE Healthcare). Computed DWI ($b = 1500 s/mm^2$) was generated from two b values of 0 and 800 s/mm^2 on the workstation (Ziostation2; Ziosoft, Tokyo, Japan).

Results

Histopathological findings

All 10 tumors were solid, round-shaped masses without capsule, and were relatively ill-defined borders compared to leiomyomas (Fig. 1). The tumors consisted of two components: abundant tubules of varying size and shape that are lined by flat or cuboidal tumor cells situated between fascicles of smooth muscle cells; reactive smooth muscle hypertrophy. These two components were distributed in concentric circles (5 lesions) or randomly (5 lesions) (Figs. 1 and 2). In 5 concentric lesions, abundant tubules were situated peripherally (4 lesions) (Fig. 3) or centrally (1 lesion) (Fig. 4).

MR imaging findings

Clinical and MR imaging findings are summarized in Table 1. All 10 tumors exhibited as outer-myometrial round solid masses, and no predominantly cystic mass was observed. The maximum diameter of the tumor, which was measured by MR imaging, was 22–50 mm (mean, 33 mm). Co-existing leiomyomas were demonstrated in 6 of 9 patients.

T2-weighted imaging

All 10 lesions showed heterogeneous signal intensity with admixture of partially ill-defined slight high-intensity areas and well-defined myoma-like low-intensity areas on T2-weighted images (Figs. 1–7). Peripheral ring-like high-intensity area was observed on T2-weighted images in 4

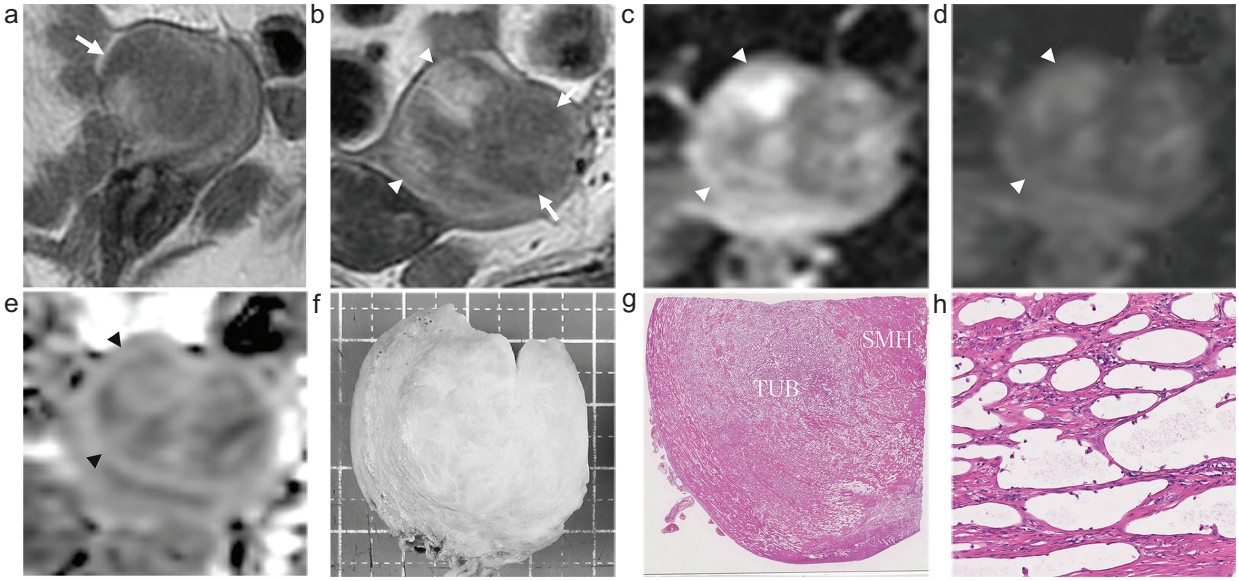

Fig. 1 A 54-year-old woman with uterine adenomatoid tumor (lesion 4). (**a**) A solid tumor of 36 mm in size (arrow) located in the outer myometrium was revealed on sagittal T2-weighted image. (**b**) The tumor was consisted with well-demarked myoma-like low-intensity areas (arrows) and relatively ill-demarcated slight high-intensity areas (arrowheads) on T2-weighted image. (**c**) High-intensity areas on T2-weighted image also showed high intensity (arrowheads) on DWI ($b = 800$ s/mm^2). (**d**) High-intensity areas on DWI showed signal decrease (arrowheads) on computed DWI ($b = 1500$ s/mm^2). (**e**) High-intensity areas on DWI showed relatively high ADC value (1.51×10^{-3} mm^2/s) (arrowheads) on corresponding ADC map. (**f**) Resected specimen showed a solid, round-shaped, relatively ill-defined mass without capsule. (**g**) A slide image section under loupe magnification (hematoxylin and eosin staining) showed the random admixture two components: areas of abundant tubules of varying size (TUB), and areas of smooth muscle hypertrophy (SMH). (**h**) A high magnification of the area of TUB (hematoxylin and eosin staining) showed the tubules lined by flat or cuboidal tumor cells situated between fascicles of smooth muscle cells. ADC, apparent diffusion coefficient; DWI, diffusion-weighted imaging; SMH, smooth muscle hypertrophy; TUB, abundant tubules.

lesions (Figs. 3 and 5), whereas one lesion showed central high-intensity area in the low-intensity mass (Fig. 4). The other 5 lesions appeared as the masses with a random mixture of high and low signal intensity areas. These results reflected the admixture of areas of smooth muscle hypertrophy showing low signal intensity with well-defined margins, and areas of abundant tubules showing relatively high signal intensity with ill-defined margins on T2-weighted images.

DWI

DWI was obtained in 9 lesions in 8 patients. Areas of abundant tubules also showed high signal intensity on DWI ($b = 800$ s/mm^2), in which signal decrease was observed on computed DWI ($b = 1500$ s/mm^2) with relatively high ADC (high-intensity areas: 1.40–1.73, mean 1.54×10^{-3} mm^2/s; low-intensity areas: 1.14–1.43, mean 1.33×10^{-3} mm^2/s) in 6 of 9 lesions, suggesting T2 shine-through effect (Figs. 1 and 2). And in 3 of these 6 lesions, peripheral ring-like high-intensity area was observed on DWI, which also showed ring-like high intensity on T2-weighted images (Fig. 3). In the other 3 of 9 lesions, 2 lesions did not contain high signal intensity areas on DWI and showed mainly low intensity on T2-weighted images. On the pathological specimen, small tubules were seen scattered within the area of dense smooth muscle hypertrophy resulting in T2 blackout effect. The other one lesion showed high intensity both on DWI and computed DWI ($b = 1500$ s/mm^2) with relatively low ADC (1.14×10^{-3} mm^2/s). Abundant tubules with less obvious cystic dilatation were mixed with smooth muscle hypertrophy on the pathological specimen, which might cause water diffusion restriction (Fig. 6).

Intra-tumoral hemorrhage

High-intensity hemorrhagic foci on T1-weighted image were not observed in all 10 lesions. SWAN was obtained in 6 lesions in 5 patients, and showed small signal voids reflecting hemorrhage in one lesion with hyalinized necrosis possibly due to partial ischemic changes.

Contrast enhancement

Post-contrast T1-weighted image was obtained in 7 lesions in 6 patients including 6 lesions in 5 patients with dynamic contrast-enhanced study. The degree of contrast enhancement on post-contrast T1-weighted images was either lower than ($n = 3$) or equal to higher than that of the myometrium ($n = 1$). The other three lesions showed heterogeneous contrast enhancement: the admixture of lower areas and equal to higher areas compared with that of the myometrium.

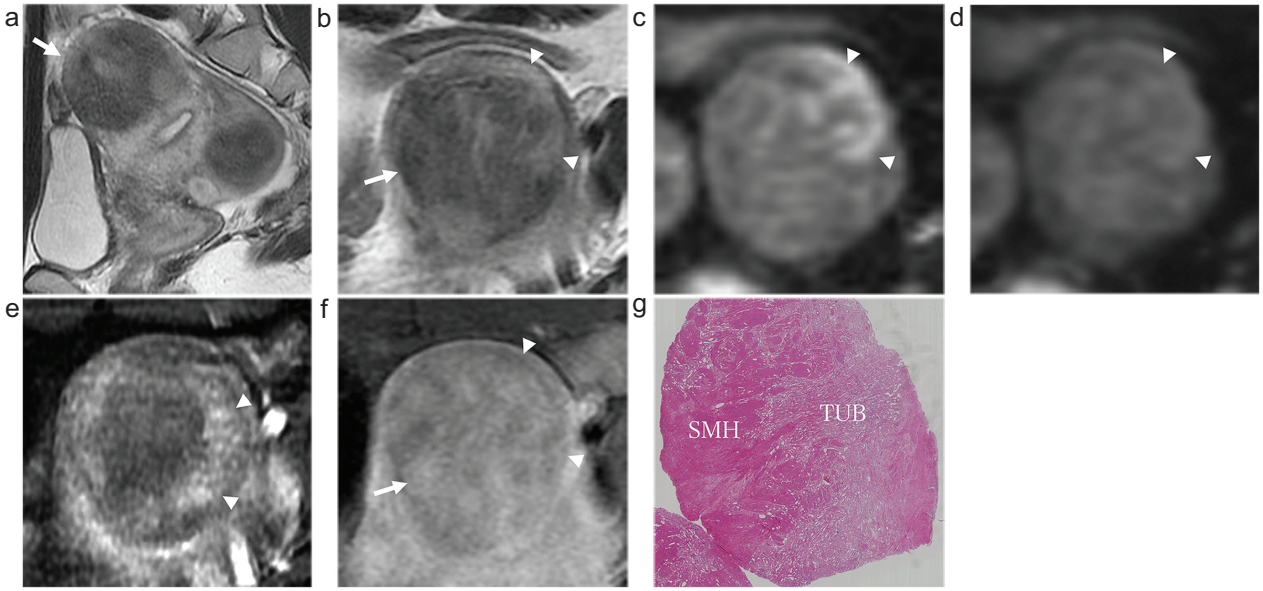

Fig. 2 A 29-year-old woman with uterine adenomatoid tumor (lesion 1). (**a**) A solid tumor of 50 mm in size located in the outer myometrium (arrow) was revealed on sagittal T2-weighted image. (**b**) The tumor was consisted with well-demarked myoma-like low-intensity areas (arrow) and relatively ill-demarcated slight high-intensity areas (arrowheads) on T2-weighted image. (**c**) High-intensity areas on T2-weighted image also showed high intensity (arrowheads) on DWI (b = 800 s/mm^2). (**d**) High-intensity areas on DWI showed signal decrease (arrowheads) on computed DWI (b = 1500 s/mm^2). (**e**) Early intense contrast-enhanced areas (arrowheads) were observed dominantly within the high-intensity areas on T2-weighted image on dynamic contrast-enhanced MRI. (**f**) The degree of contrast-enhancement on post-contrast T1-weighted image tended to be weaker (arrowheads) in high-intensity areas on T2-weighted image and stronger (arrow) in low-intensity areas on T2-weighted image. (**g**) A slide image section under loupe magnification (hematoxylin and eosin staining) showed the random admixture two components: areas of TUB of varying size and areas of dense SMH. DWI, diffusion-weighted imaging; SMH, smooth muscle hypertrophy; TUB, abundant tubules.

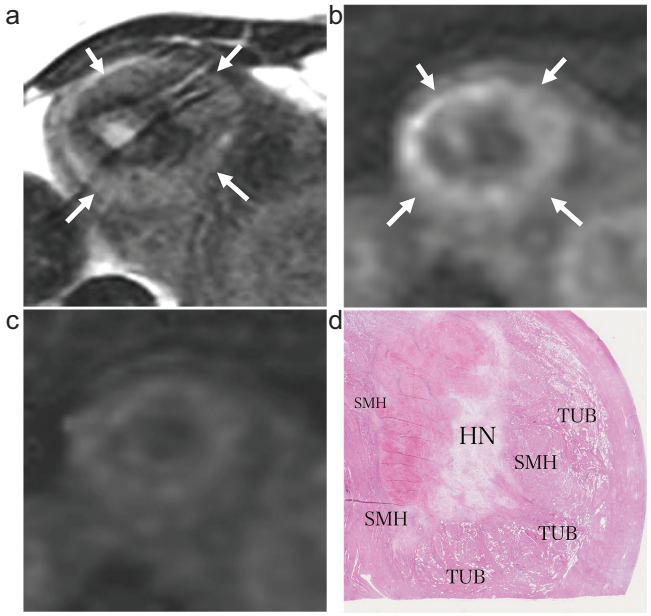

Fig. 3 A 45-year-old woman with uterine adenomatoid tumor (lesion 2). (**a**) A solid tumor of 32 mm in size located in the outer myometrium was revealed on T2-weighted image. The tumor showed target-like appearance: peripheral ring-like high-intensity area (arrows) and central doughnut-like low-intensity area with intense high-intensity hole. (**b**) Peripheral ring-like high-intensity area on T2-weighted image also showed high intensity (arrows) on DWI (b = 800 s/mm^2). (**c**) Peripheral ring-like high-intensity area on DWI showed signal decrease on computed DWI (b = 1500 s/mm^2). (**d**) A slide image section under loupe magnification (hematoxylin and eosin staining) showed outer areas with TUB and inner areas of SMH distributed in concentric circles. The center of the mass contained hyalinized necrosis (HN) with hemorrhage possibly due to partial ischemic changes. DWI, diffusion-weighted imaging; HN, hyalinized necrosis; SMH, smooth muscle hypertrophy; TUB, abundant tubules.

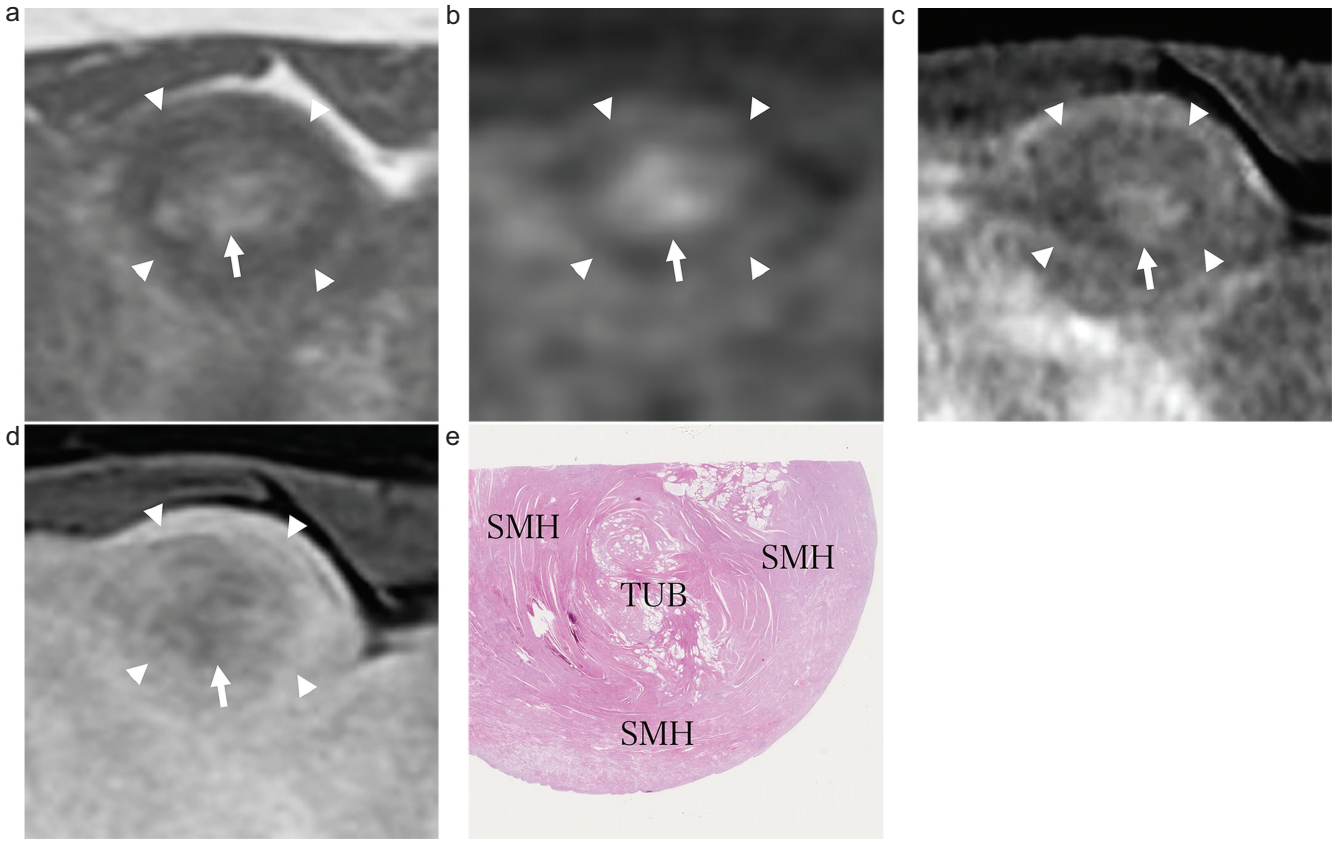

Fig. 4 A 45-year-old woman with uterine adenomatoid tumor (lesion 3). (**a**) A solid tumor of 38 mm in size located in the outer myometrium was revealed on T2-weighted image. The tumor showed target-like appearance: peripheral ring-like low-intensity area (arrowheads) and central high-intensity area (arrow). (**b**) Central high-intensity area on T2-weighted image showed high intensity (arrow) on DWI (b = 800 s/mm^2). (**c**) Early intense contrast-enhanced area (arrow) was observed within the central high-intensity area on T2-weighted image on dynamic contrast-enhanced MRI. (**d**) The degree of contrast-enhancement in peripheral area was stronger (arrowheads), whereas that in central area was weaker (arrow) on post-contrast T1-weighted image. (**e**) A slide image section under loupe magnification (hematoxylin and eosin staining) showed outer areas of SMH and inner areas with TUB distributed in concentric circles. DWI, diffusion-weighted imaging; SMH, smooth muscle hypertrophy; TUB, abundant tubules.

The degree of contrast enhancement on post-contrast T1-weighted images tended to be weaker in the high-intensity areas on T2-weighted images possibly reflecting abundant unenhanced tubules and small cysts (Figs. 2 and 4). In 6 lesions with dynamic contrast-enhanced study, all lesions contained some early intense contrast-enhanced areas dominantly within the high-intensity areas on T2-weighted images but rarely within the myoma-like low-intensity areas on T2-weighted images (Figs. 2, 4, and 7). Areas showing intense contrast enhancement equal to or greater than the outer myometrium in the early phase at visual assessment were considered as hypervascular.

Discussion

Mitsumori et al. reported two cases of uterine adenomatoid tumor mimicking leiomyoma on MR images.[7] These tumors appeared as well-circumscribed low-intensity masses relative to the myometrium on T2-weighted images. Meng et al. reported MR imaging findings of 26 cases with uterine adenomatoid tumor, including 24 solid and 2 cystic tumors. The 24 solid tumors included 18 homogeneous low-intensity masses and 6 low-intensity masses with patchy slight high--intensity areas. The margins were well-defined in 21 lesions and ill-defined in 3 lesions. They stated that it was difficult to differentiate solid adenomatoid tumors and leiomyomas based solely on MR imaging appearance.[9] In our study, all 10 lesions showed heterogeneous signal intensity with admixture of slight high-intensity areas and low-intensity areas on T2-weighted images. Adenomatoid tumor is composed of mesothelial origin tubules of varying size with smooth muscle hypertrophy.[1–6] Areas containing small cystic dilatations of abundant tubules may increase the signal intensity on T2-weighted images, whereas areas of smooth muscle hypertrophy may show low signal intensity like leiomyoma. Nogales et al. reviewed the pathological findings of 60 uterine adenomatoid tumors including 48 nodular, solid tumors.[3] The growth pattern of the tubular tumor cells

Table 1 Case summary

No.	Age (years)	Symptoms	Size (mm)	MRI Tesla	T2WI Signal	Margin	DWI_{800} Signal	ADC (x 10^{-3} mm^2/s)			$cDWI_{1500}$ Signal	DCE-MRI Early CE	Gd-T1WI CE degree	SWAN Signal voids	T1WI High foci	Co-exist Myoma
								Whole	DWI-high	DWI-low						
1	29	Dysmenorrhea	50	1.5	High & low random	Well w/ ill	High & low random	1.43	1.42	1.36	Decreased	Peripheral	Weak & intense	ND	–	+
2	45	Anemia	32	1.5	High ring & central low	Well w/ ill	High ring & central low	1.56	1.61	1.14	Decreased	Peripheral	Weak & intense	+	–	+
3*			38		Low ring & central high	Well w/ ill	Low ring & central high	1.40	1.73	1.39	Decreased	Central	Weak & intense	–	–	
4	54	None	36	1.5	High & low random	Well w/ ill	High & low random	1.46	1.51	1.43	Decreased	ND	ND	–	–	–
5	40	Amenorrhea	33	1.5	High ring & central low	Well w/ ill	High ring & central low	1.43	1.40	1.39	Decreased	Peripheral	Weak	–	–	–
6	39	Dysmenorrhea Menorrhagia	22	3	High ring & central low	Well w/ ill	High ring & central low	1.48	1.57	1.28	Decreased	Whole	Intense	ND	–	+
7	42	Menorrhagia	45	1.5	High & low random	Well w/ ill	Low	1.36	N/A	N/A	Stable	ND	ND	ND	–	+
8	39	Dysmenorrhea	25	3	High & low random	Well w/ ill	High	1.14	N/A	N/A	Stable	ND	Weak	–	–	–
9	43	Menorrhagia Anemia	28	1.5	High ring & central low	Well w/ ill	ND	ND	ND	ND	ND	ND	ND	ND	–	+
10	43	Menorrhagia Anemia	18	1.5	High & low random	Well w/ ill	Low	1.04	N/A	N/A	Stable	Peripheral	Weak	–	–	+

*Lesion 3 is the same patient with lesion 2. ADC, apparent diffusion coefficient; $cDWI_{1500}$, computed diffusion-weighted imaging (b = 1500 s/mm^2); CE degree, the degree of contrast enhancement; DCE-MRI, dynamic contrast-enhanced magnetic resonance imaging; DWI_{800}, diffusion-weighted imaging (b = 800 s/mm^2); Early CE, early contrast enhancement; Gd-T1WI, gadolinium-enhanced T1-weighted imaging; N/A, not available; ND, not done; SWAN, susceptibility-weighted sequence; T2WI, T2-weighted imaging; well w/ill, well-defined mass with partially ill-defined margins.

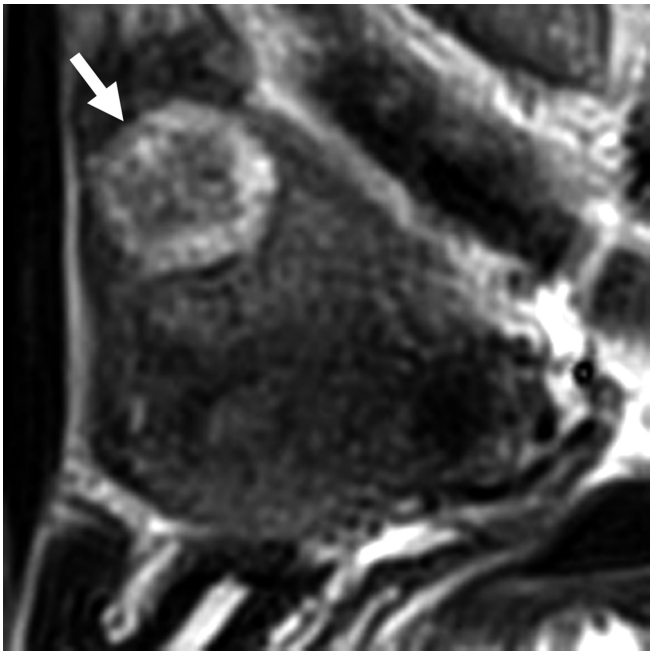

Fig. 5 A 43-year-old woman with uterine adenomatoid tumor (lesion 9). A solid tumor of 28 mm in size located in the outer myometrium was revealed on sagittal T2-weighted image. The tumor showed target-like appearance: peripheral ring-like high-intensity area (arrow) and central low-intensity area.

consisted of an organized nodular, concentrically arranged, targetoid structures in 22% of cases, and randomly oriented in 60% of cases. In our series, abundant tubules were distributed in concentric circles in 5 lesions including 1 centrally situated lesion and 4 peripherally situated lesions. On T2-weighted images, the lesion with centrally situated abundant tubules appeared as a low-intensity mass with central high-intensity mimicking leiomyoma with degeneration, whereas the lesion with peripherally situated abundant tubules appeared as a ring-like high-intensity mass with central low intensity. This peripheral ring-like high intensity on T2-weighted images is rarely observed in leiomyomas and may be suggestive of adenomatoid tumors. Myometrial high signal intensity rim due to edema surrounding leiomyomas on T2-weighted images is well known; however, peripheral ring-like high signal intensity due to degeneration of leiomyoma is not reported as common MRI findings.[12]

There are no reports on DWI findings of uterine adenomatoid tumors. Tsili et al. reported MR imaging findings including DWI of a paratesticular adenomatoid tumor arising from the tunica albuginea.[13] The tumor showed low intensity on T2-weighted images and DWI ($b = 900$ s/mm^2) with low ADC (0.86×10^{-3} mm^2/s), possibly due to T2 blackout effect by abundant fibrous components. In our study, 6 of 9 lesions with DWI ($b = 800$ s/mm^2) showed heterogeneous high and low intensity. The high-intensity areas showed relatively high ADC and signal decrease on computed DWI with high b-value ($b = 1500$ s/mm^2). In these lesions, the high-intensity areas on DWI also showed high intensity on T2-weighted images, and it is considered that the high intensity on DWI is due to T2 shine-through effect reflecting abundant tubules. The low-intensity areas on DWI corresponded to the low-intensity areas on T2-weighted images reflecting smooth muscle hypertrophy. In the other three lesions, two lesions which exhibited mainly low intensity on T2-weighted images showed no diffusion restriction but one lesion contained high intensity both on DWI and high b-value computed DWI with relatively low ADC value suggesting diffusion restriction.

Intra-tumoral hemorrhagic necrosis is suggestive finding for uterine sarcomas.[14] In this study, most lesions showed no intra-tumoral hemorrhage, which may be compatible with benign tumor. SWAN revealed small amount of hemorrhagic change in one lesion with hyalinized necrosis possibly due to partial ischemic changes, and the hemorrhage was considered as secondary change.

The degree of contrast enhancement on post-contrast T1-weighted images tended to be weaker in the high-intensity areas on T2-weighted images possibly due to unenhanced small cystic spaces formed by the dilatation of abundant tubules. Mitsumori et al. reported two lesions appeared low intensity relative to the myometrium on post-contrast T1-weighted images.[7] Meng et al. reviewed 24 solid lesions and the degree of enhancement was either lower than ($n = 18$) or equal to that of the myometrium ($n = 6$), and speculated that the lower enhancement was probably due to the reduction of interstitial vessel resulting from the lacunar-like arrangement of tumor cells.[9] In our study, early intense contrast-enhanced areas on dynamic contrast-enhanced study were observed dominantly within the high-intensity areas on T2-weighted images probably reflecting neovascularization due to abundant tumor cells. On the other hand, the low-intensity areas on T2-weighted images tended to show weaker enhancement on the early phase and stronger enhancement on post-contrast T1-weighted images. This might be because areas of reactive smooth muscle hypertrophy may not be accompanied with neoplastic neovascularization. Because ordinary leiomyomas show low intensity on T2-weighted images and hypervascularity on dynamic contrast MRI,[15,16] hypovascularity of myoma-like low-intensity areas in adenomatoid tumor may be a clue for the differential diagnosis. Leiomyoma with hyaline degeneration also shows low signal intensity on T2-weighted images and does not show intense contrast enhancement in the early phase of dynamic contrast MRI; however, it is not contrast enhanced on post-contrast T1-weighted images. In the current study, dynamic contrast MRI was performed in only 6 lesions, and verification of this finding by additional case numbers is considered necessary.[15]

The retrospective nature and small population are limitations in this study. Use of multiple field strength and MR

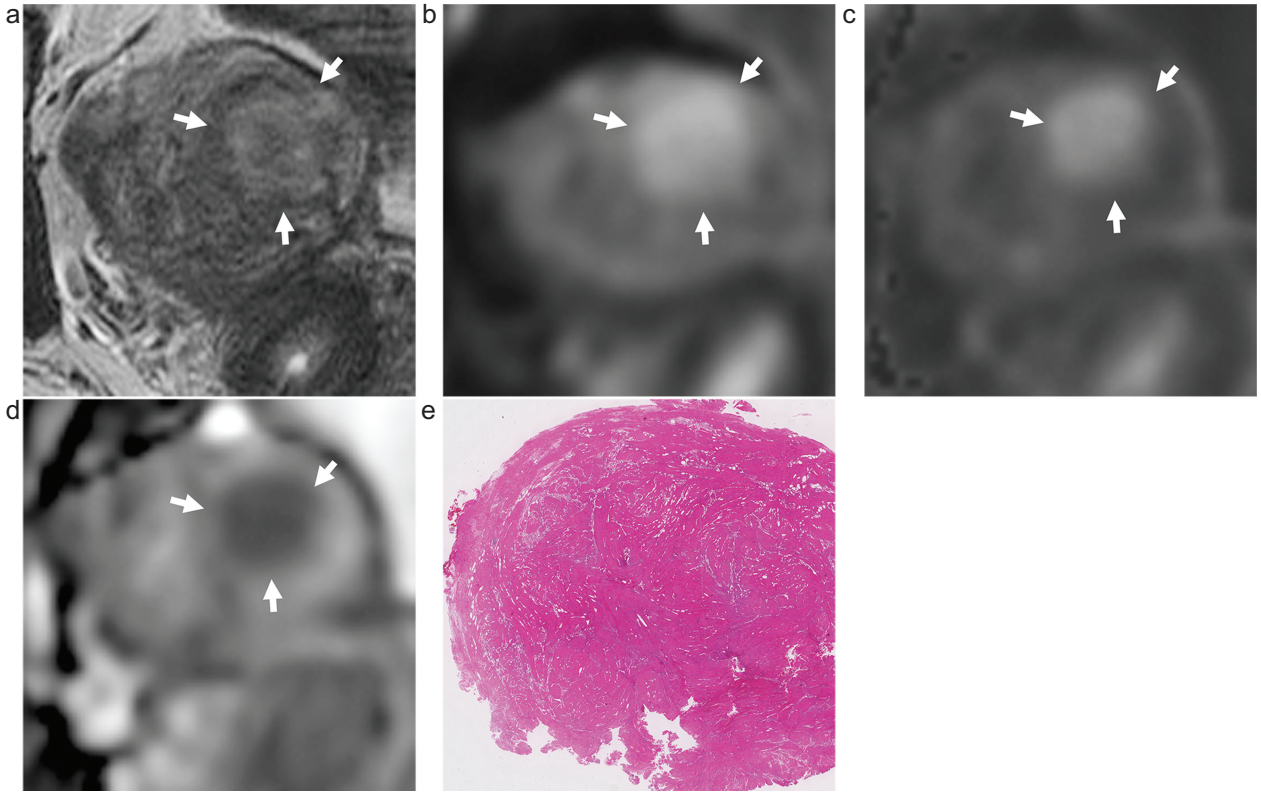

Fig. 6 A 39-year-old woman with uterine adenomatoid tumor (lesion 8). (**a**) A solid tumor of 25 mm in size was revealed on T2-weighted image. The tumor (arrows) was consisted with myoma-like low-intensity areas and relatively ill-demarcated slight high-intensity areas. (**b**) The tumor showed high intensity (arrows) on DWI ($b = 800$ s/mm^2). (**c**) The tumor also showed high intensity (arrows) on computed DWI ($b = 1500$ s/mm^2). (**d**) The tumor showed relatively low ADC value (1.14×10^{-3} mm^2/s) (arrows) on corresponding ADC map. (**e**) A slide image section under loupe magnification (hematoxylin and eosin staining) showed abundant tubules with less obvious cystic dilatation were mixed with smooth muscle hypertrophy. ADC, apparent diffusion coefficient; DWI, diffusion-weighted imaging.

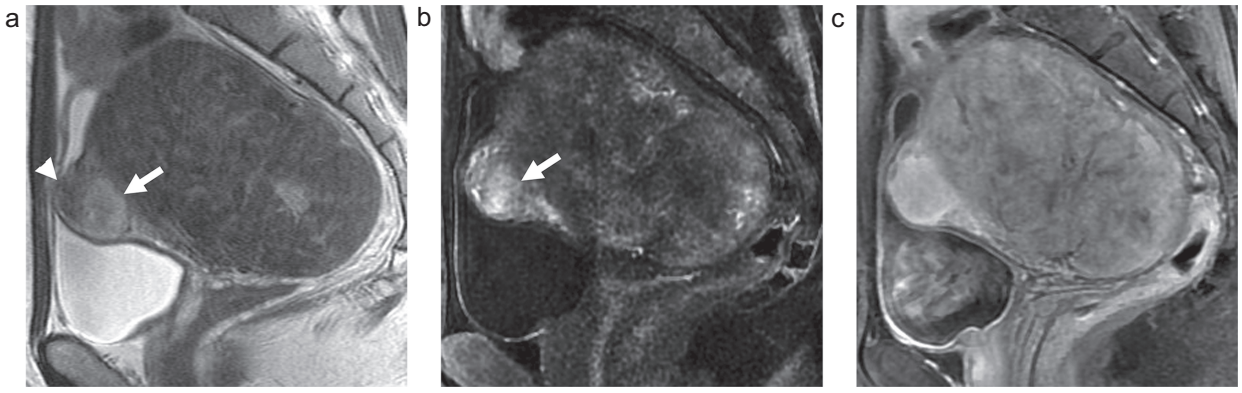

Fig. 7 A 39-year-old woman with uterine adenomatoid tumor (lesion 6). (**a**) A solid tumor of 22 mm in size located in the outer myometrium was revealed on sagittal T2-weighted image. The tumor was consisted with myoma-like low-intensity area (arrowhead) and slight high-intensity area (arrow). (**b**) Early intense contrast-enhancement (arrow) was observed mainly in the high-intensity area on T2-weighted image on dynamic contrast-enhanced MRI. (**c**) The tumor was totally well contrast-enhanced on post-contrast T1-weighted image.

devices may also be a limitation. Further studies in larger populations to verify the results are needed. Another limitation of this study is case selection bias. In this study, we included relatively large lesions for which MR images could be correlated with pathology and did not include small lesions found incidentally in hysterectomy specimens. However, small lesions are unlikely to be clinically problematic to differentiate from leiomyomas.

Conclusion

Uterine adenomatoid tumors may mimic leiomyomas on MR imaging; however, uterine outer myometrial mass with admixture of well-defined low-intensity areas and ill-defined high-intensity areas on T2-weighted images may be suggestive of adenomatoid tumor. Especially, peripheral ring-like high intensity on T2-weighted images and DWI may also be suggestive. Relatively high ADC and absence of intratumoral hemorrhage may suggest its benignity. Dynamic contrast-enhanced MR study may be helpful for the differentiation from leiomyoma.

Conflicts of Interest

The authors declare that they have no conflicts of interest.

References

1. Golden A, Ash JE. Adenomatoid tumors of the genital tract. Am J Pathol 1945; 21:63–79.
2. Quigley JC, Hart WR. Adenomatoid tumors of the uterus. *Am J Clin Pathol* 1981; 76:627–635.
3. Nogales FF, Isaac MA, Hardisson D, et al. Adenomatoid tumors of the uterus: an analysis of 60 cases. *Int J Gynecol Pathol* 2002; 21:34–40.
4. Sangoi AR, McKenney JK, Schwartz EJ, Rouse RV, Longacre TA. Adenomatoid tumors of the female and male genital tracts: a clinicopathological and immunohistochemical study of 44 cases. *Mod Pathol* 2009; 22:1228–1235.
5. Quick CM, Solomon DA. Tumours of the peritoneum: mesothelial tumours: adenomatoid tumour, In: The WHO Classification of Tumours Editorial Board, ed. WHO classification of tumours: Female genital tumours, 5th ed. Lyon:World Health Organization, 2020; 177–178.
6. Oliva E, Zaloudek CJ, Soslow RA. Mesenchymal tumors of the uterus: miscellaneous mesenchymal tumors and conditions: adenomatoid tumor, In: Kurman RJ, Ellenson LH, Ronnett BM Blaustein's pathology of the female genital tract, 7th ed. Cham:Springer, 2019; 621–622.
7. Mitsumori A, Morimoto M, Matsubara S, Yamamoto M, Akamatsu N, Hiraki Y. MR appearance of adenomatoid tumor of the uterus. *J Comput Assist Tomogr* 2000; 24:610–613.
8. Kim JY, Jung KJ, Sung NK, Chung DS, Kim OD, Park S. Cystic adenomatoid tumor of the uterus. *Am J Roentgenol* 2002; 179:1068–1070.
9. Meng Q, Zeng Q, Wu X, et al. Magnetic resonance imaging and pathologic findings of 26 cases with uterine adenomatoid tumors. *J Comput Assist Tomogr* 2015; 39:499–505.
10. Alkatout I, Bojahr B, Dittmann L, et al. Precarious preoperative diagnostics and hints for the laparoscopic excision of uterine adenomatoid tumors: two exemplary cases and literature review. *Fertil Steril* 2011; 95:1119.e5–1119.e8.
11. Sakurai N, Yamamoto Y, Asakawa Y, Taoka H, Takahashi K, Kubushiro K. Laparoscopically resected uterine adenomatoid tumor with coexisting endometriosis: case report. *J Minim Invasive Gynecol* 2011; 18:257–261.
12. Mittl RL Jr., Yeh IT, Kressel HY. High-signal-intensity rim surrounding uterine leiomyomas on MR images: pathologic correlation. *Radiology* 1991; 180:81–83.
13. Tsili AC, Argyropoulou MI, Giannakis D, Sofikitis N, Tsampoulas K. Conventional and diffusion-weighted magnetic resonance imaging findings of benign fibromatous paratesticular tumor: a case report. *J Med Case Rep* 2011; 5:169.
14. Takeuchi M, Matsuzaki K, Harada M. Clinical utility of susceptibility-weighted MR sequence for the evaluation of uterine sarcomas. *Clin Imaging* 2019; 53:143–150.
15. Shimada K, Ohashi I, Kasahara I, et al. Differentiation between completely hyalinized uterine leiomyomas and ordinary leiomyomas: three-phase dynamic magnetic resonance imaging (MRI) vs. diffusion-weighted MRI with very small b-factors. *J Magn Reson Imaging* 2004; 20:97–104.
16. Thomassin-Naggara I, Daraï E, Nassar-Slaba J, Cortez A, Marsault C, Bazot M. Value of dynamic enhanced magnetic resonance imaging for distinguishing between ovarian fibroma and subserous uterine leiomyoma. *J Comput Assist Tomogr* 2007; 31:236–242.